THIN FILM DEPOSITION • PLASMA PROCESSING • VACUUM INSTRUMENTATION

vacuum & coating TECHNOLOGY

SEPTEMBER 2004

Characterizations of Electron Beam-Generated Plasmas for Materials Processing

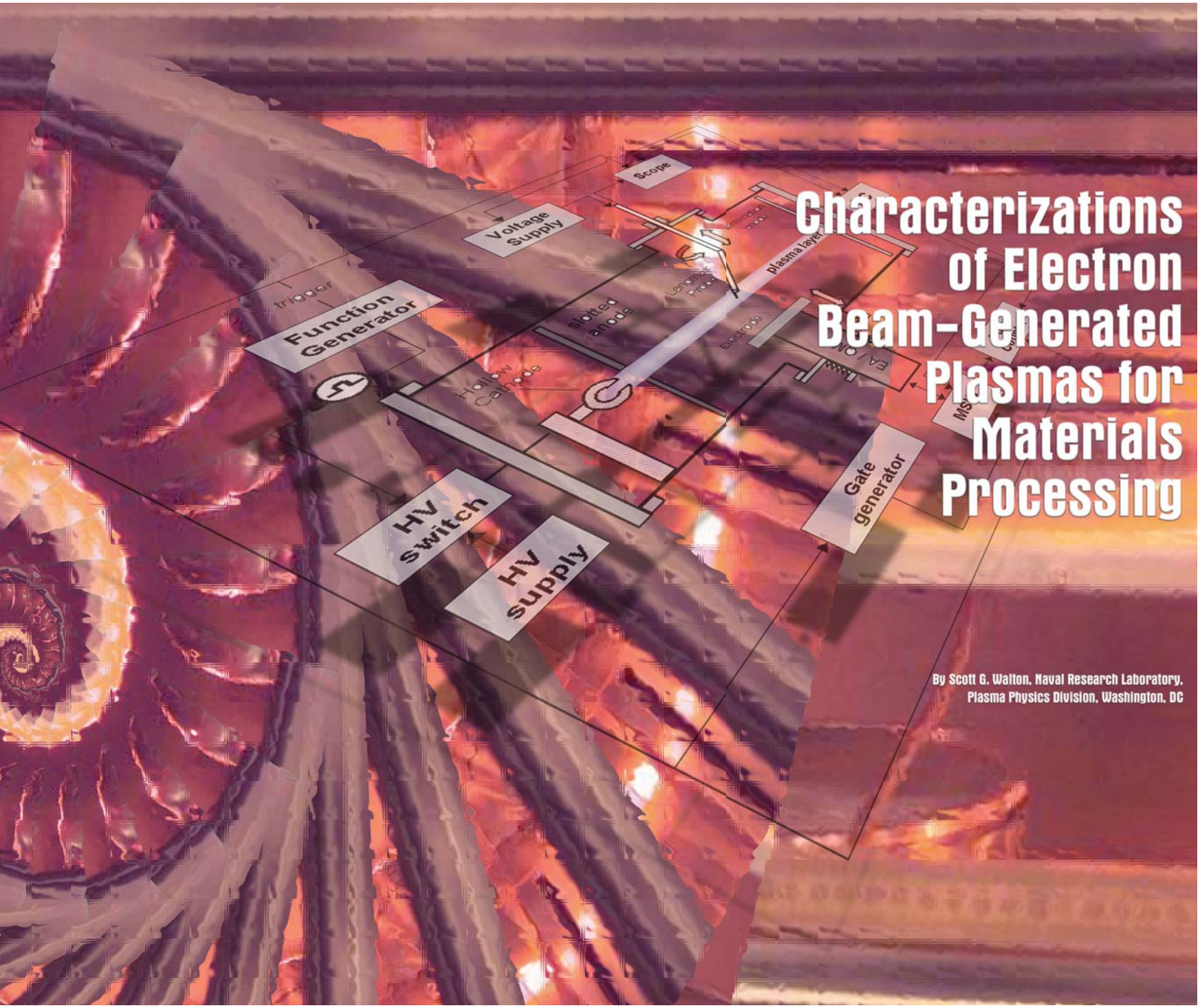

Characterizations of Electron Beam–Generated Plasmas for Materials Processing

By Scott G. Walton, Naval Research Laboratory, Plasma Physics Division, Washington, DC

Scott Walton is a staff scientist in the U.S. Naval Research Laboratory's Plasma Physics Division. He came to NRL in 1998 to work on electron beam generated plasmas and materials processing as a National Research Council Postdoctoral Fellow. Prior to coming to NRL, Dr. Walton received a B.S. in physics from Bloomsburg University of Pennsylvania and M.S. and PhD degrees in physics from The College of William and Mary. He is a member of the Society of Vacuum Coaters and serves as assistant chair of the Plasma Processing TAC.

In plasma-based processes ranging from etching to deposition, characterizing the flux of reactive species at the substrate is an essential component in surface engineering. Characterizing the bulk plasma properties is equally critical, since both the plasma density (n_p) and electron temperature (T_e) directly influence the ion flux at surfaces adjacent to the plasma. The plasma density determines the total number of ions incident to surfaces, while the electron temperature determines the plasma potential (V_p), thereby dictating the ion energies at grounded surfaces. The chemical pathways available for a given gas composition are also determined by T_e and influence the production of ions and reactive neutrals. Generally, n_p and T_e are influenced by the input power, gas pressure, constituent gas species, and by the relative location of electrodes and chamber walls. In terms of materials processing, it is critical to know the relationship between these input parameters, the bulk plasma properties, and their effect on the substrate surface in order to have a reasonable understanding of system operation and optimization.

Typically, continuous plasma production is used, which operates at a steady state based on the various input parameters. However, modulating plasma production adds additional capabilities that may be used to further enhance process control and quality. The "steady state" in pulsed production, if achieved at all, rep-

resents only a fraction of the processing time. Over the course of one period, the plasma exhibits distinct phases that can lead to unique and potentially useful changes in the flux of species at processing surfaces. While benefits do exist, pulsed plasmas require additional care when characterizing the bulk properties and surface flux composition.

The Naval Research Laboratory has developed a materials processing system based on a plasma source driven by electron beam ionization [1]. The system relies on a magnetically confined, modulated multi-keV electron beam to ionize a background gas, producing a plasma with several unique features. The resulting system is well suited for a number of applications, including nitriding [2], etching [3, 4], deposition [5], and polymer modification [5].

This article discusses experiments to characterize electron beam-generated plasmas with the goal of developing a complete spatio-temporal description of the system. Langmuir probe measurements were used to determine bulk plasma properties and the flux of ion species was measured using a dual energy analyzer/mass spectrometer. The diagnostics were also designed to provide spatial resolution and to correlate the measured bulk properties with the flux of ions at the electrode. Because the plasma is modulated, careful attention is required to properly determine the temporal dependencies. The selected results presented here serve to illustrate both the unique features of the system as well as the means to regulate the flux of ion species in processing applications.

BACKGROUND

The features that separate electron beam-generated plasmas from conventional sources (ICP's, ECR's, rf diodes, etc.) are largely derived from the method of plasma generation: ionization by a high-energy electron beam. First, scalability is straightforward, since the electron beam cross-section relies on the length and width of electron beam source while the range or length of the beam scales with operating pressure and beam energy. Furthermore, gas ionization is limited to the electron beam volume and when the electron beam is collimated by a magnetic field; the result is a well-defined and localized source. The plasma characteristics are essentially uniform over the source volume but vary, sometimes strongly, with distance from the beam edge.

Perhaps the most remarkable feature of these plasmas is the low average electron temperatures ($T_e \approx 0.3$ - 1.5 eV) [6], which arise from the fact that electron beam-driven ionization precludes the need for externally applied electric fields. In other sources, these fields are used to heat the plasma electrons so that a sufficient number of electrons are energetic enough to sustain the plasma [7]. In the absence of electric fields, the plasma electrons are allowed to cool electrostatically or by inelastic collisions with the background gas. A low T_e leads to a low plasma potential (V_p), so ions incident to surrounding walls and substrates exhibit comparatively low energies (< 6 eV) when the surfaces are grounded [8]. A low T_e also makes available a different set of electron-neutral reaction rates when compared to higher temperature plasmas.

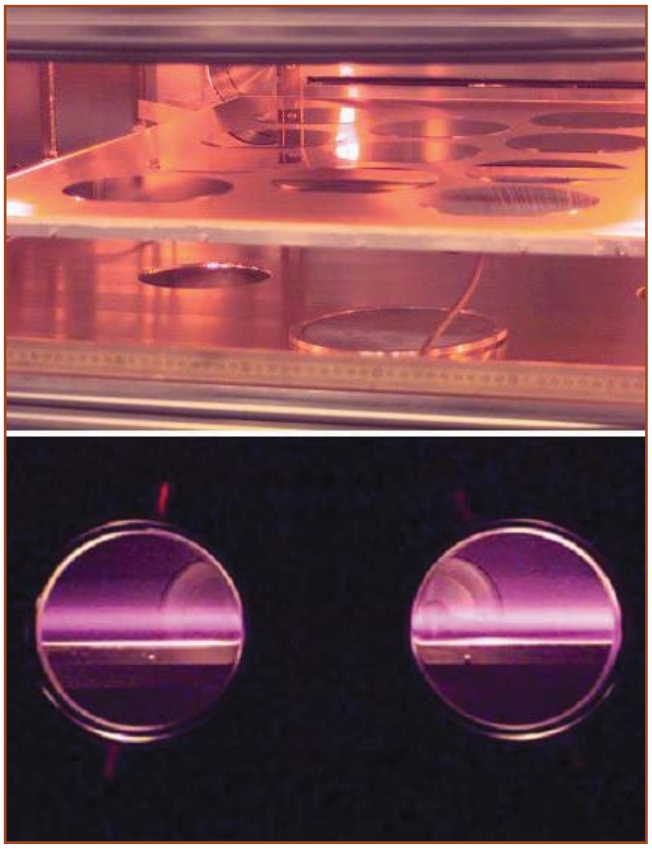

Figure 1. Photographs of the large area processing system. (a) Inside of system showing large area stage loaded with eleven 6" silicon wafers. (b) The system during operation as seen through two 8" ports with the large area stage located just below the plasma layer.

Finally, species production by high-energy (> 2 keV) electron beams is largely determined by the relative concentrations of the working gas [9], since the primary ionization cross sections are similar for most gases. This is in contrast to most conventional sources where species production strongly favors those with the lowest energy threshold. It is also important to recognize that the ionization cross section dominates all reactions at high energies and so little energy is lost through excitation and dissociation.

EXPERIMENTAL APPARATUS

Chamber and Plasma Production

The electron beam source has been operated in a number of chambers [6, 8, 10] and is transferable between systems without significant differences in operation. The largest system currently in operation is shown in **Figure 1**, where the plasma source was scaled to treat surface areas up to ½ m^2 (1m × ½ m). Different scales aside, all chambers are similar to the chamber used in this work (**Figure 2**). The electron beam is produced by a linear hollow cathode [3] operating at multi-kilovolts. The emergent beam passes through a slot in a grounded anode in front of the hollow cathode before termination at a second anode located further downstream. The electron beam volume between the two anodes defines the ionization source volume, with the dimensions set by the slot size and the anode-to-anode length.

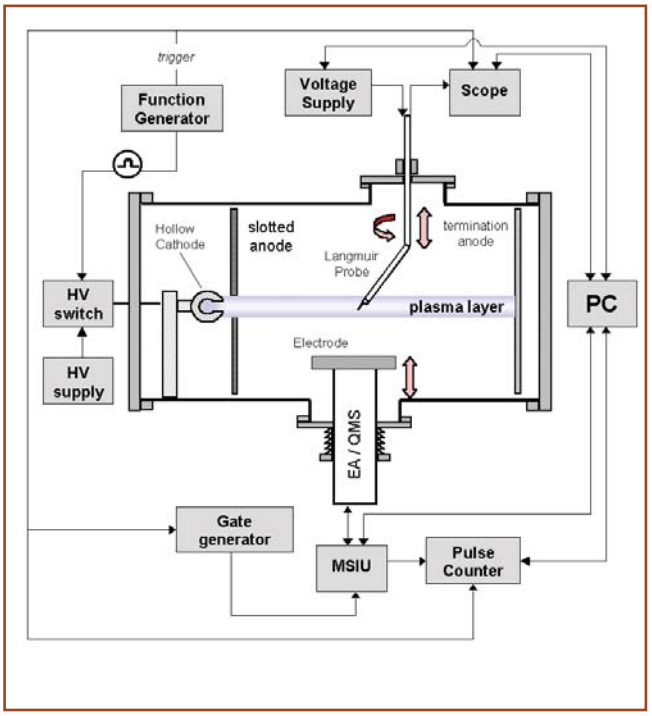

Figure 2. Simplified diagram of the diagnostic system.

Beam spreading via collisions with neutral is largely eliminated by a longitudinal magnetic field.

For the measurements described here, the linear hollow cathode was driven by a – 2kV pulse, generating a sheet-like electron beam with energy commensurate with the applied bias. The pulse widths were varied between 1 and 6 ms with duty ratio between 10% and 50%. The slot dimensions were 1 cm x 25 cm and the anode-to-anode distance is 43 cm, with the beam thickness of 1 cm maintained by a 150 Gauss magnetic field.

Plasma Diagnostics

Ion energy distributions and fluxes were measured at the center of a grounded 5.7 cm diameter stainless steel electrode using a Hiden EQP 300 Plasma Probe (**Figure 2**). Ions enter the EQP through a 20 μm diameter aperture located in the center of the electrode and are first energy selected by an electrostatic energy analyzer (EA) and then mass filtered by a quadrupole mass spectrometer (QMS). The energy analyzer has a fixed resolution ($\Delta E/E_t$), and the transmission energy (E_t) was adjusted to provide an uncertainty in energy of approximately ± 0.15 eV. The EQP has not been calibrated to determine the absolute flux of each species, so the intensity of the measured signal is reported in arbitrary units.

Temporally resolved ion energy distributions were measured by gating the output of the EQP such that the distributions were accumulated only during the specified time window. For the energy-resolved ion flux measurements, the EQP passed ions of a given energy, and the signal output was monitored by a dual channel, pulse counter operated in a scanning gate mode. The real-time output of the EQP was accumulated during a gate that was scanned with respect to the beam front. For both measurements, the signal was accumulated over several hundred pulses to achieve a reasonable signal-to-noise ratio.

The plasma parameters, T_e, n_p, and V_p were determined using a Langmuir probe [6,7] that was mounted on a multi-motion feedthrough and heated to reduce surface contaminants. Time-resolved probe characteristic data was accumulated by stepping the probe voltage in discrete intervals and recording the current as a function of time at each voltage. The characteristic I-V trace can then be generated at any given time. The values of T_e and n_p are derived from a best fit of the I-V trace to a Maxwellian electron energy distribution.

All data acquisition is computerized. The software to control the EQP is provided by the vendor, while LabView© programs were written to automate the time-resolved flux and Langmuir probe measurements. Additional analysis programs were used to batch-process raw data when needed.

RESULTS

Pure Gases: Temporal Characterization

Plasmas generated in pure gas backgrounds were compared to develop a fundamental understanding of plasma production and to this end, plasmas produced in 50 mTorr argon and nitrogen where studied. The pulse widths were set to 6 ms and 3 ms for argon and nitrogen respectively, and a 10% duty cycle.

The ion energy distributions measured at the EQP electrode located 2.5 cm from the beam axis are shown in **Figure 3**. These distributions were accumulated over the latter half of each pulse to avoid any transient behavior at the beam/plasma initiation or extinction; that is, to approximate a steady state condition. The distributions illustrate the differences between the plasmas produced in each gas, with the features of interest being the mean energy (1.5-1.75 eV for N_2 species and 3.1 eV for Ar) and relative intensities (factor of 5 increase in Ar). The temporal behavior of T_e and n_p for each plasma is shown in **Figures 4** and **5**, measured with the Langmuir probe located on the axis of the electron beam and in front of the electrode.

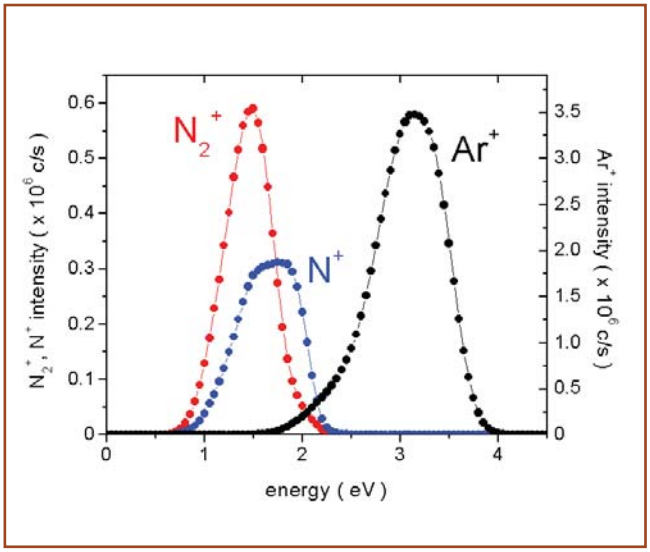

Figure 3. Ion energy distributions accumulated at an electrode located adjacent to plasmas produced in 50 mTorr of Nitrogen and Argon.

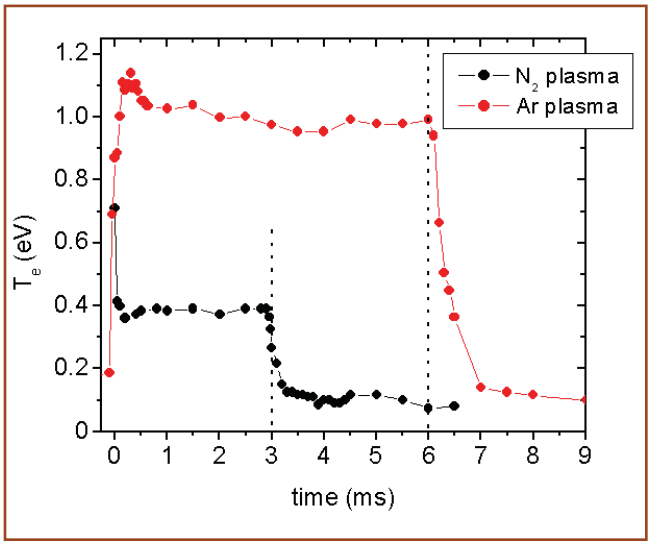

Figure 4. The on-axis electron temperature determined from Langmuir probe measurements in plasmas produced in 50 mTorr of Nitrogen and Argon.

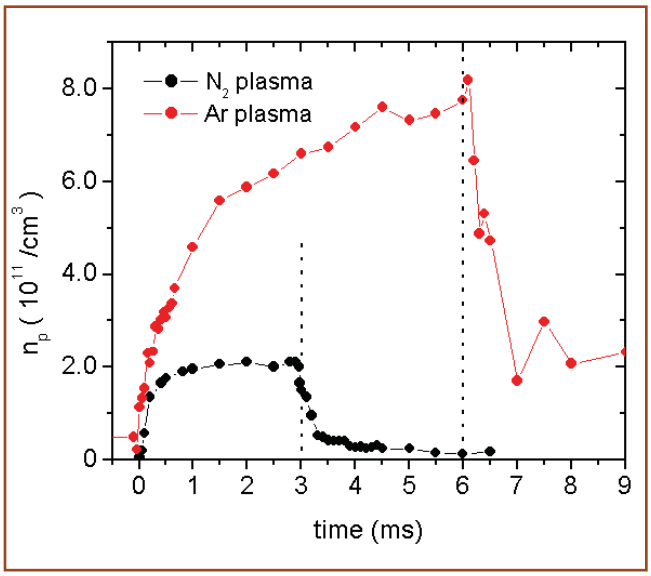

Figure 5. The on-axis plasma density determined from Langmuir probe measurements in plasmas produced in 50 mTorr of Nitrogen and Argon.

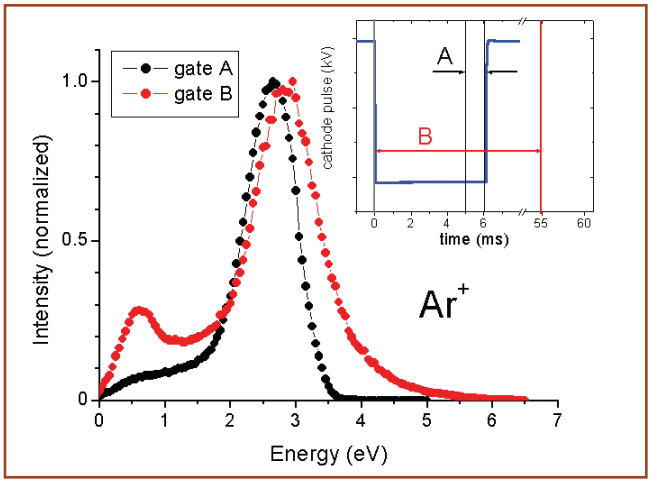

Figure 6. Ar^+ ion energy distributions measured during two separate gates; gate timings and widths are shown in the inset.

The time-dependent nature of the incident Ar^+ ion energy is indicated in **Figure 6**, which shows ion energy distributions accumulated over two different time windows. For gate A, the distribution was accumulated during a one ms window beginning at 5 ms and gate B extended from zero to 55 ms. Gate B indicates a multi-peaked, broad range of incident ion energies relative to gate A, suggesting a strongly time-dependent ion energy. This temporal evolution in ion energy is illustrated in **Figure 7**. For these measurements, the energy analyzer was set to pass Ar^+ ions of a discrete energy, and the flux was accumulated during a 30 μs gate that was scanned in steps of 50 μs up to 9 μs. For times greater than 9 μs, the 30 μs gate was stepped in 200 μs increments. The *total* Ar^+ ion flux can be approximated by the sum of the energy-resolved fluxes, and those results are shown in **Figure 8** on both linear and logarithmic (inset) scales. To ensure the correct representation, the energy-resolved fluxes must span the entire range of incident energies (see the gate B distributions from **Figure 6**) and be partitioned equally, with proper attention given to the passband of the energy analyzer. In this case, 14 separate energy-resolved fluxes spanning the range from 0 to 6.5 eV were taken in 0.5 eV increments. Given the energy uncertainty (±

Table 1. The results of Langmuir probe measurements at arbitrary locations along the electron beam axis. The plasma potential (V_p), electron temperature (T_e), and plasma density (n_p) are listed for a grounded and biased termination anodes.

	Grounded Anode			25 V Anode Bias			50 V Anode Bias		
Location (arbitrary)	V_p (V)	T_e (eV)	n_p x 10^{11} (cm^{-3})	V_p (V)	T_e (eV)	n_p x 10^{11} (cm^{-3})	V_p (V)	T_e (eV)	n_p x 10^{11} (cm^{-3})
1	1.9	0.5	1.8	25.9	0.4	2.0	50.7	0.4	1.9
2	2.2	0.6	2.4	25.9	0.6	2.2	51.0	0.6	2.2
3	2.2	0.6	2.1	25.7	0.6	1.8	50.6	0.5	1.6
4	1.9	0.5	2.0	25.7	0.6	2.0	50.5	0.5	1.4

0.15 eV), the measured flux shown in **Figure 8** was a reasonable representation of the total ion flux. Note that the zero of the abscissa is defined by the front of the hollow cathode pulse, so the data offset was due to the time-of-flight in the EQP.

Pure Gases: Spatial Characterization

Shown in **Figure 9** are T_e and n_p as a function of distance from the beam axis for a plasma produced in 50 mTorr of argon. For these measurements, the EQP electrode was fixed at 2 cm from the beam axis and the Langmuir probe was scanned along a line normal to the center of the electrode. The data was taken at 5 ms into a 6 ms pulse. The electron beam width is ≈ 1.0 cm and is indicated by the shaded area.

The uniformity of the bulk plasma properties along the length of the plasma was evaluated by rotating the Langmuir probe through an arc along the beam axis. Those results are shown in **Table 1** for several operating conditions. The location of the probe is somewhat unknown, however locations one and four were within 2 cm of the slotted and termination anodes respectively. Location three was above the EQP electrode and location 2 was between the slotted anode and the EQP electrode. Included in **Table 1** are analogous measurements where the plasma potential was elevated by biasing the termination anode, which is equivalent to negatively biasing the substrate to increase the ion energies [12].

Gases Mixtures: Spatio-temporal Characterization

Plasmas used in our laboratory to nitride stainless steel [2] were subjected to the same measurement techniques, and the results are shown in **Figures 10** and **11**. For this experiment, the total pressure was 160 mTorr (12 % Ar) and the period was 2 ms with a 50% duty cycle. The three species shown (N_2^+, N^+, Ar^+), represent 99% of all measured species, and although not shown, ion energies were comparable to those in pure nitrogen. For the temporally-resolved fluxes in **Figure 10**, the electrode was positioned at a distance of 3.5 cm from the beam axis and a 10 μs gate was stepped in 10 μs increments. The relative ion flux as a function of electrode distance from the beam is shown in **Figure 11**. For these results, the flux for each species is determined by integrating the energy distributions accumulated over the entire period. The total flux is the sum of all species shown and is normalized to its maximum value for all locations. Of interest here is the relative intensity of each species, which was found by normalizing the flux of each species to the total ion flux.

DISCUSSION

Basic Characteristics

The use of high-energy electron beams to ionize gas eliminates the role of plasma electrons in sustaining the plasma. That is not to say they have no influence on the plasma properties. Indeed, many of the unique features of electron beam produced plasmas follow from the unusually low electron

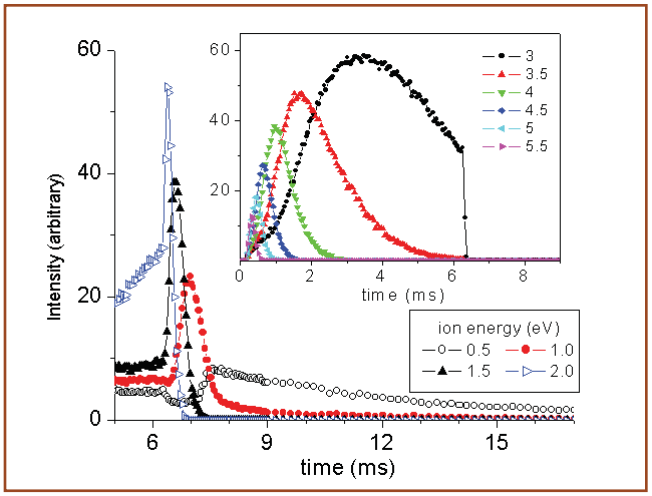

Figure 7. Energy-resolved Ar^+ ion fluxes. The higher energy ions are shown in the inset.

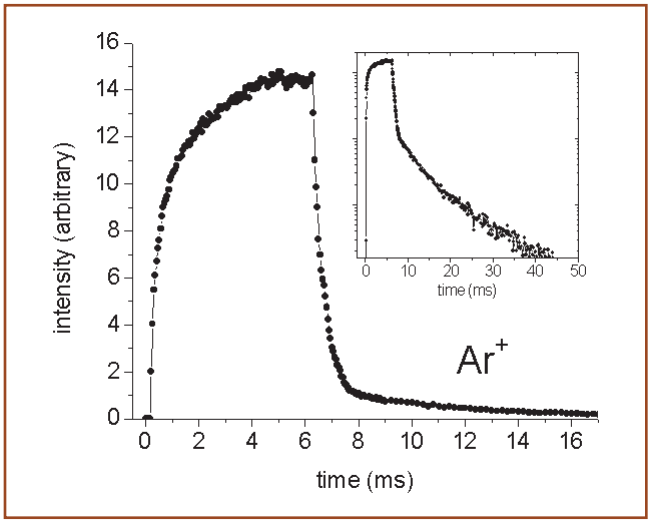

Figure 8. Total Ar^+ ion flux. The inset shows the same data using a logarithmic scale.

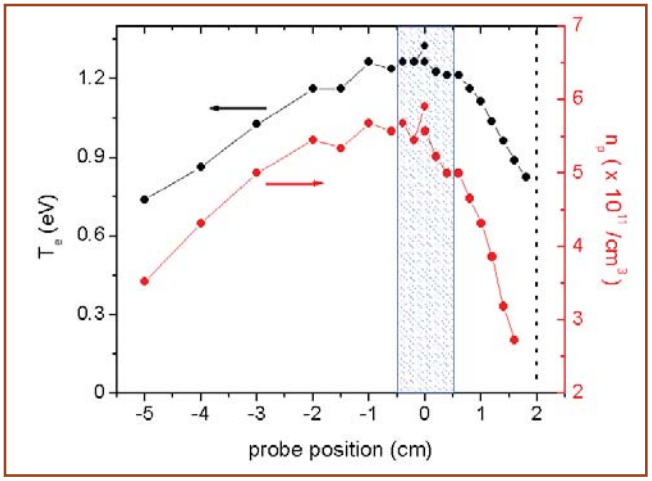

Figure 9. Plasma density and electron temperature as a function of position. The vertical line indicates the position of the electrode and the shaded areas represents the approximate electron beam width. Inset: The total Ar^+ ion flux as a function of electrode position.

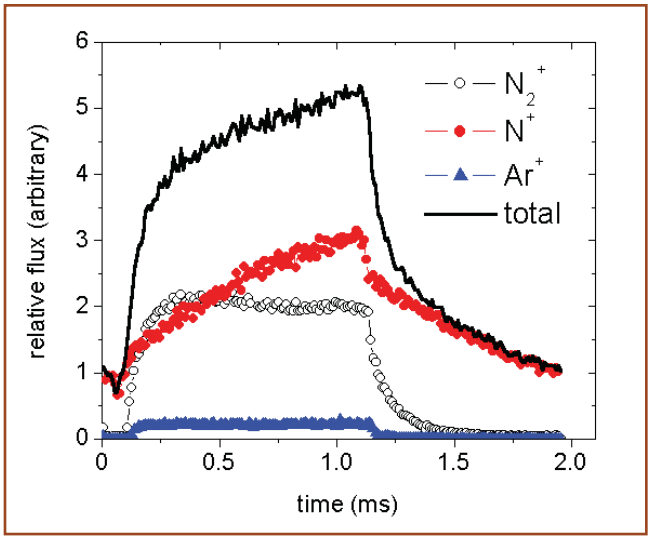

Figure 10. Time-resolved ion fluxes in plasma produced in nitrogen mixtures.

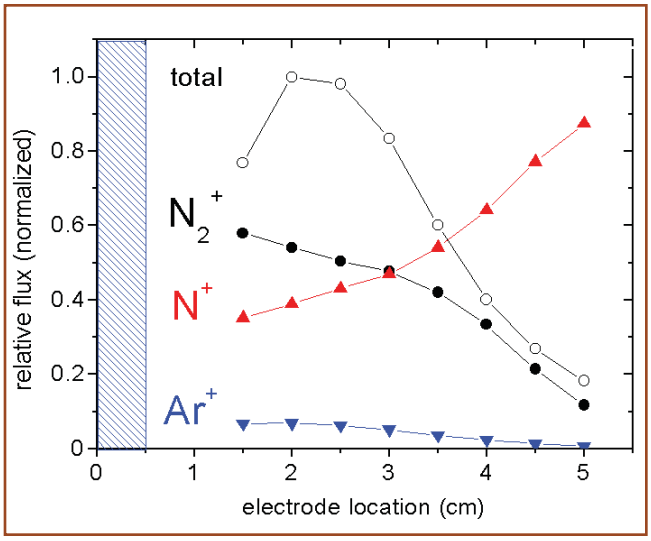

Figure 11. Spatially-resolved ion fluxes in plasma produced in nitrogen mixtures.

temperature. Take the ion energy distributions in **Figure 3**, which span only a few eV and are several times lower than those found in other plasma sources with comparable densities. Such an attribute is useful in, for example, the treatment of polymers by plasma eliminating the detrimental effects of excessive ion energies [13].

In conventional sources, externally applied electric fields are used to drive the plasma by elevating the energy of a small fraction of the plasma electrons above the ionization potential of the background gas. Heating from the external fields is balanced mainly by cooling from inelastic electron-neutral collisions. In electron beam-generated plasmas, the electric fields are (usually) absent and thus T_e is low. In nitrogen for example, vibrational excitations have a large cross-section and a threshold of about 0.3 eV [14], so T_e will be comparable to the threshold value. T_e will be similarly low in other molecular gases due to the availability of low-energy excitational levels. By contrast, the lowest argon metastable level lies at about 11.5 eV and so electron cooling is predominately electrostatic, resulting in higher electron energies (**Figure 4**) and thus greater ion energies (**Figure 3**).

In addition to setting the plasma potential, T_e strongly affects electron reactions. In nitrogen plasmas, dissociative electron-ion recombination ($e^- + N_2^+ \rightarrow 2N$) is significant because the rate ($kr = 4x10^{-8}\ [T_e]^{-0.4}\ cm^3/s$) becomes large at low electron energies [15]. This reaction quickly destroys molecular ions but not atomic ions; the relative density of N^+ compared to N_2^+ is thus higher than from beam ionization alone [16]. By comparison, recombination in argon is insignificant at these pressures. Ar^+ is mainly lost via diffusion to the walls, a slower process that increases the buildup and decay times and is largely responsible for the higher plasma density.

The characteristics of electron beam generated plasmas will clearly vary with gas types. Generally, molecular gases have an abundance of low-energy excitational levels (vibrational and rotational) and will be rich in chemical pathways. Noble gases, like argon, have fewer pathways and have excitation levels that are much larger fractions of their ionization energies. As a result, plasmas produced in molecular gases have lower electron temperatures, ion energies, and plasma densities.

Temporal Characteristics

The temporal behaviors of n_p and T_e for plasmas produced in argon and nitrogen are qualitatively similar and illustrate the general trends in pulsed plasma production. In particular, T_e is high initially and then decreases to nearly constant values before collapsing in the afterglow. The plasma density, on the other hand, exhibits a smooth increase to its steady state value before collapsing in the afterglow. The behavior of T_e and n_p can be correlated to similar time dependencies seen in the ion fluxes at electrodes located adjacent to the plasma.

The evolution in T_e leads directly to a time-varying ion energy. For example, the variation in the Ar^+ ion energy distributions seen in **Figure 6** follows T_e, which varies significantly over the course of one period but remains essentially constant during the steady state period. The evolution in ion energy is seen in **Figure 7**, where ions with energies < 3.0 eV dominate the afterglow while ions with energies > 3.0 eV dominate while the beam is on. This transition from high to low ion energy parallels the changes in T_e.

In a similar way, the total ion flux of **Figure 8** parallels the density measurements of **Figure 5**. Although the Langmuir probe is less sensitive than the flux measurements, the plasma appears to persist for 10's of milliseconds in the afterglow of argon, indicative of diffusive losses rather than electron-ion recombination.

From these results, three general plasma phases are evident: initiation, steady state, and afterglow. The initiation is characterized by high electron temperatures and low densities, which lead

to a low flux of high-energy ions. The steady state is characterized by nearly constant ion energies and fluxes that approximate those found in continuous plasma production. The afterglow is characterized by a collapse in both T_e and n_p and thus in a decrease in ion flux and energies. The transition between the initiation and steady-state phases is typically smoother than the transition to the afterglow. As noted, this behavior is not specific to argon, nor is it limited to this method of plasma production; the overall progression is comparable to global models [17], simulations [18], and experimental results [19] for pulsed plasma production using other sources.

Spatial Characteristics

The results of **Figure 9** illustrate the localized nature of the plasma source, in that n_p, T_e, and the ion flux decrease with distance from the beam. The asymmetry in T_e and n_p is thought to be related to the system geometry, i.e. a small electrode located near the plasma layer and an opposing wall located far from the plasma layer [20]. As expected, the total ion flux to the EQP electrode varies with distance similar to n_p. The maximum ion energies measured during the steady-state period (**Figure 6**) are consistent with the value of T_e near the EQP electrode. The ability to regulate the ion flux (and energy) as a function of distance from the ionization source provides a useful 'knob' in process control.

A uniform flux of ions and radicals over the entire substrate surface is predicated on the ability to produce a uniform plasma, which is difficult in large area processing. The results of **Table 1** indicate a reasonable consistency in the bulk plasma properties along the axis of the electron beam in nitrogen. The data also suggest that the plasma potential can be elevated uniformly over the length of the beam and although not shown here, the incident ion energies are in agreement with the measured plasma potential [21]. These results indicate that electron beams can produce uniform, large area plasmas with controllable ion energy and fluxes. This is a useful first step to large area processing, although other challenges remain, including uniformity in gas flow.

Production in Gas Mixtures

The spatio-temporal evolution in plasmas produced in mixtures of Ar and N_2 is not unlike plasmas produced in pure gases when considering the total flux, but the interest and utility lie in the evolution of each species. Here again, gas-phase reactions play an important role. Consider the afterglow (**Figure 10**), where N_2^+ and Ar^+ ions decay rapidly after the beam is extinguished. As previously mentioned, N_2^+ is rapidly destroyed via dissociative electron-ion recombination. Ar^+ ions are mainly destroyed through charge exchange reactions ($Ar^+ + N_2 \rightarrow Ar + N_2^+$) and N^+ ions are lost through diffusion and thus decay slowly. In fact, the flux of N^+ does not fully decay before the next pulse begins, resulting in a variable but continuous ion flux. These reactions are also responsible for the dominance of N^+ ions at large distances from the beam shown in **Figure 11**. Note that the rise in the total ion flux for small distances is related to the previously discussed symmetry issues of the system. Nonetheless, the spatial profile of the *total* ion flux varies slowly with distance, whereas the relative fluxes vary strongly.

The results in Ar/N_2 mixtures highlight features that are beneficial to stainless steel nitriding and should be useful in other processes as well. As in pure nitrogen, the destruction of N_2^+ creates two N atoms. The exact density of radicals has not been measured but should be comparable to the plasma density [2]. Hence, the flux of molecular and atomic ions as well as radicals will vary in both time and distance. The relative fluxes can therefore be adjusted by changing the plasma period, pulse width, duty cycle, electrode location, or combinations thereof.

Summary

The diagnostics and measurements in this work were aimed at characterizing pulsed, electron beam-generated plasmas. The results demonstrate the unique properties of these plasmas, which are characterized by high plasma densities and low electron temperatures, and can thus produce a large flux of low-energy ions at adjacent surfaces. The fluxes vary in time because the plasma is pulsed and vary with distance from the electron beam because of the well-localized nature of the source. This combination of features provides access to processing conditions unattainable with other plasma sources. It is straightforward to tailor the relative flux of useful reactive species by adjusting the relative gas concentrations and/or substrate position with respect to the electron beam. Similarly, pulsing the plasma leads to a variable ion and radical flux that can be regulated by changing the pulse width or duty ratio. This control over the flux coupled with the relative ease in scaling to treat large area substrates makes these plasma potentially useful in a wide variety of processing applications.

Acknowledgements

This work was supported by the Office of Naval Research and profits from the continuing efforts of Drs. Darrin Leonhardt, Richard Fernsler, and Robert Meger of NRL and from the work Dr Christopher Muratore (American Society of Engineering Education).

References

[1] For an overview of electron beam-generated plasmas see: D. Leonhardt, Vacuum Technology and Coatings, 2 (11), 24-31 (2002) and the references therein.

[2] C. Muratore, D. Leonhardt, S.G. Walton, D.D. Blackwell, R.F. Fernsler, and R.A. Meger, Surf. Coat and Technol. (2004) (in press); C. Muratore, S.G. Walton, D. Leonhardt, R.F. Fernsler, D.D. Blackwell, and R.A. Meger, J. Vac. Sci. Technol. A, 22 (4), 1530 (2004).

[3] D. Leonhardt, C. Muratore, S.G. Walton, D.D. Blackwell, R.F. Fernsler, R.A. Meger, Surf. Coat and Technol. 177-178, 682 (2004).

For Free Literature, Circle 29

Ferro Tec

With over 20 years experience in the electron beam field and the most advanced and reliable products on the market, Ferrotec makes process control issues a thing of the past.....

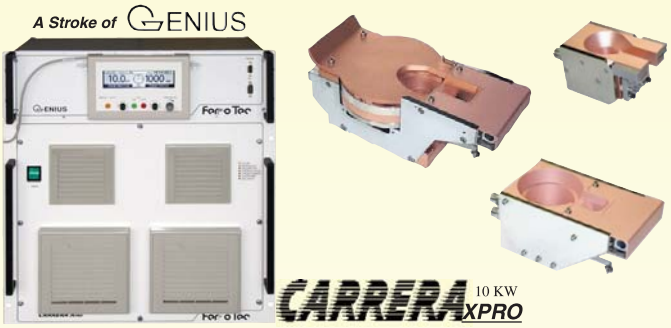

- The innovative *Genius* controller takes evaporation control to the next generation
- Ferrotec's electron beam sources revolutionize the concept of evaporation
- The *Carrera* and the all New *Carrera XPRO* solid state power supplies lead the industry in arc suppression and reliability

Nashua, NH

603-883-9800 *www.ferrotec.com* sales@ferrotec.com

Next Generation Trapping for a New Generation of Processes

Now, more than ever, avoiding costly unscheduled system down time can mean the difference between profit and loss. Meet the challenge with the new MV MULTI-TRAP®, designed for today's more demanding manufacturing processes. We built on the solid performance and reputation of our original MV MULTI-TRAP® line, increasing the cooling surface area by over 200% and adding 25% greater capacity.

MV PRODUCTS
A Division of Mass-Vac, Inc.

247 Rangeway Road • PO Box 359, North Billerica, MA 01862-0359
TEL 978-667-2393 FAX 978-671-0014 www.massvac.com

For Free Literature, Circle 30

[4] D. Leonhardt, S.G. Walton, C. Muratore, R.F. Fernsler, and R.A. Meger, J. Vac. Sci. and Technol. A (2004) (in press).

[5] C. Muratore, S.G. Walton, D. Leonhardt, R.F. Fernsler, and R.A. Meger, Society of Vacuum Coaters 47th Annual Technical Conference Proceedings, (2004) in press.

[6] D. Leonhardt, S.G. Walton, D.D. Blackwell, W.E. Amatucci, D.P. Murphy, R.F. Fernsler, and R.A. Meger, J. Vac. Sci. Technol. A 19(4), 1367, (2001); S.G. Walton, D. Leonhardt, R.F. Fernsler, R.A. Meger, D.D. Blackwell and C. Muratore, Society of Vacuum Coaters 46th Annual Technical Conference Proceedings, 447 (2003).

[7] For a good review of plasma fundamentals see: K. Becker and A. Belkind, Vacuum Technology and Coatings, 4 (9), 30 (2003), 5 (1), 30 (2004), 5 (5), 34 (2004).

[8] S.G. Walton, D. Leonhardt, D.D. Blackwell, R.F. Fernsler, D.P. Murphy, and R.A. Meger, J. Vac. Sci. Technol. A 19(4), 1325-1329 (2001).

[9] S.G. Walton, D. Leonhardt, R.F. Fernsler, and R.A. Meger, Society of Vacuum Coaters 45th Annual Technical Conference Proceedings, 378 (2002).

[10] S.G. Walton, D. Leonhardt, D.D. Blackwell, R.F. Fernsler, D.P. Murphy, and R.A. Meger, Phys. Rev E 65, 046412 (2002).

[11] D. Leonhardt, W. Amatucci, and G. Gatling, NRL Memorandum Report NRL/MR/6750—04-8761.

[12] J.W. Coburn and E. Kay, J. Appl. Phys. 43 4695 (1972).

[13] J.M. Grace and L.J. Gerenser, J. Dispersion Sci. Technol. 24, 305 (2003).

[14] J. Schulze, Phys. Rev. 135, A983 (1964); A.G. Engelhardt, A.V. Phelps, C.G. Risk, Ibid A1566.

[15] F.J. Mehr and M.A. Biondi, Phys. Rev. 181, 264 (1969).

[16] For a 2 keV electron beam, N^+ production is roughly 20% that of N_2^+: S.P. Slinker, A.W. Ali, and R.D. Taylor, J. Appl. Phys. 67, 679 (1990).

[17] M.A. Lieberman and S. Ashida, Plasma Sources Sci. Technol. 5, 145-158 (1996).

[18] P. Subramonium and M.J. Kushner, Appl. Phys. Lett. 79, 2145-2147 (2001).

[19] M.V. Malyshev, V.M. Donnelly, J.I. Colonell, and S. Samukawa, J. Appl. Phys. 86, 4813-4820 (1999).

[20] This assumption is supported additional measurements that show on-axis density was influenced by the electrode position when the electrode is close to the plasma layer. This effect is also seen in the total flux of **Figure 11**, where the flux maximum is not located a the closest position.

[21] S.G. Walton, C. Muratore, D. Leonhardt, R.F. Fernsler, D.D. Blackwell, and R.A. Meger, Surf. Coat. Technol., 186 (1-2), 40 (2004).